

Multimodal Fusion Learning with Dual Attention for Medical Imaging

Joy Dhar¹ Nayyar Zaidi² Maryam Haghghat³ Puneet Goyal^{1,6} Sudipta Roy⁴
Azadeh Alavi⁵ Vikas Kumar¹

¹Indian Institute of Technology Ropar ²Deakin University ³Queensland University of Technology ⁴Jio Institute, India
⁵RMIT University ⁶NIMS University, Jaipur, India

Abstract

Multimodal fusion learning has shown significant promise in classifying various diseases such as skin cancer and brain tumors. However, existing methods face three key limitations. First, they often lack generalizability to other diagnosis tasks due to their focus on a particular disease. Second, they do not fully leverage multiple health records from diverse modalities to learn robust complementary information. And finally, they typically rely on a single attention mechanism, missing the benefits of multiple attention strategies within and across various modalities. To address these issues, this paper proposes a dual robust information fusion attention mechanism (DRIFA) that leverages two attention modules – i.e., multi-branch fusion attention module and the multimodal information fusion attention module. DRIFA can be integrated with any deep neural network, forming a multimodal fusion learning framework denoted as DRIFA-Net. We show that the multi-branch fusion attention of DRIFA learns enhanced representations for each modality, such as dermoscopy, pap smear, MRI, and CT-scan, whereas multimodal information fusion attention module learns more refined multimodal shared representations – improving the network’s generalization across multiple tasks and enhancing overall performance. Additionally, to estimate the uncertainty of DRIFA-Net predictions, we have employed an ensemble Monte Carlo dropout strategy. Extensive experiments on five publicly available datasets with diverse modalities demonstrate that our approach consistently outperforms state-of-the-art methods. The code is available at <https://github.com/misti1203/DRIFA-Net>.

1. Introduction

Recent advancements in machine learning (ML) for medical imaging analysis, particularly in cancer classification, have transformed healthcare practices enabling quick and

cost-effective decision-making for physicians and potentially saving lives [10]. It is important to note that there are various imaging modalities prevalent in medical domain such as dermoscopy, pap smear, MRI, and CT scans – and are crucial for detecting cancers like skin, cervical, brain tumors, and lung cancer. Existing methods for handling multiple modalities relies on building models on single modality and then leverage techniques such as transfer learning (TL), feature fusion, attention mechanisms, etc. to exploit knowledge of each model [1,4,7,12,14,19,21,25,29,31,33,39–41]. However, reliance on single-modal learning approaches often results in sub-optimal performance due to inefficient feature extraction and noise in the data, leading to over-fitting as well. How to learn an effective model that can leverage various modalities – also known as *Multimodal fusion learning* (MFL), has been an open question in machine learning. Multimodal fusion learning integrates information from multiple modalities to enhance representation and therefore improve predictive performance [16]. It aims to address various challenges faced by single-modal models by learning shared representations from diverse modalities.

In the last few years, attention-based models have rose to popularity which automatically learn the importance of any individual token (i.e., element of interest) [38], and multimodal fusion learning has not been any exception.

E.g., [6,9,11,13,15,27] are some notable attention-based works that have been developed to learn robust representations from medical imaging modalities. However, these approaches face significant challenges. Firstly, they often have limited capacity to learn shared complementary information leading to sub-optimal performance. Also, their focus on specific a modality such as MRI, PET, and SPECT for brain disorders or dermoscopy for skin cancer restricts their generalizability. Secondly, they typically rely on single attention mechanisms, hence do not avail the opportunity to utilize multiple attention strategies to independently enhance multimodal representation learning across different modalities. These limitations underscore the need for more

robust methodology capable of addressing these issues.

To address these challenges, we propose a dual robust information fusion attention mechanism integrated within a deep neural network, denoted as DRIFA-Net. Our proposed multimodal fusion learning strategy incorporates two attention mechanisms: a) multi-branch fusion attention enhances representations within each modality, and b) multimodal information fusion attention enhances multimodal representations to improve our learning model’s performance.

In summary, our main contributions are as follows:

- We propose a dual robust information fusion attention mechanism to enhance MFL denoted as DRIFA-Net.
- We design a multi-branch fusion attention module (MFA) that combines the strengths of hierarchical information fusion attention and channel-wise local information attention modules to efficiently learn diverse local dependencies.
- We devise a multimodal information fusion attention (MIFA) module that incorporates global and local information fusion attention modules to effectively learn multimodal global-local dependencies.
- We conduct comprehensive comparisons with prior state-of-the-art approaches to demonstrate the effectiveness of our attention method on diverse medical imaging datasets: HAM10000 [37], SIPaKMeD [30], NickParvar [26], Lung CT-scan [2], and BraTS2020 [24].
- Finally, we employ the ensemble Monte Carlo dropout strategy to estimate uncertainty in our DRIFA-Net’s predictions.

The rest of the paper is organized as follows. We discuss related works in Section 2 followed by the proposition of our proposed method in Section 3. The experimental analysis is conducted in Section 4. We conclude in Section 5 with pointers to future works.

2. Related Works

Prior studies use various attention mechanisms with single-modal learning approaches to detect across different medical imaging modalities. E.g., in dermoscopy modality, different attention strategies [4, 12, 19, 21, 25, 29, 31, 39–41] have been employed to learn fine-grained details for skin cancer classification and segmentation tasks. For MRI modality, [3] used self-attention strategies. For pap smear and CT-scan modalities, existing works [14, 22, 23, 28, 32] primarily focused on feature fusion or TL strategies rather than attention mechanisms.

Multimodal fusion learning addresses the aforementioned limitations by enhancing modality strengths and thereby improving classification [16].

For instance, Chen et al. [8] developed a multimodal data fusion diagnosis network (MDFNet) for skin cancer classification integrating clinical images and patient data. Li et al. [20] designed a multimodal medical image fusion technique by decomposing medical images to capture rich gradients, benefiting MRI analysis. Kihara et al. [18] used a hybrid deep learning method combining paired medical images for enhanced clinical predictions. Tan et al. [36] introduced the multi-CoFusion approach, applying multimodal fusion learning for glioma grade classification and survival analysis using histopathological and mRNA data. Tabarestani et al. [35] deployed a distributed MFL approach for Alzheimer’s disease prediction using MRI and PET modalities.

In the following let us discuss attention-based approaches to MFL. Huang et al. [15] introduced a label-efficient multimodal medical imaging representation method, incorporating radiology reports and a global-local attention mechanism to learn global-local representations. Cheng et al. [9] proposed an MRI-based multimodal fusion learning approach using a hybrid CNN-Transformer for Glioma Segmentation and a multi-scale classifier for IDH genotyping on the BraTS2020 dataset. Georgescu et al. [11] devised a multimodal multi-head convolutional attention module for super-resolving CT and MRI scans. Cai et al. [6] developed a multimodal transformer with separate encoders for images and metadata fusion, using a vision transformer (ViT) and a mutual attention (MA) block to enhance feature fusion on HAM10000 [37]. He et al. [13] proposed a co-attention fusion (CAF) network for multimodal skin cancer diagnosis on the seven-point checklist dataset [17], utilizing co-attention (CA) and attention fusion (AF) blocks. Omeroglu et al. [27] developed a soft attention-based MFL network for multi-label skin lesion classification, leveraging multiple branches to learn complementary features.

3. Proposed Method

In this section, we will introduce our proposed model DRIFA-Net. The input features from m heterogeneous modalities are represented as $X = [x_1, x_2, \dots, x_m]$, and their corresponding labels $[y_1, \dots, y_t]$ – the model is expected to perform t (binary or multi-class) classification tasks. X is used as input to DRIFA-Net $\theta(\cdot)$ to learn an enhanced multimodal shared representations denoted as: $X^S = \theta(X) = [x_1^s, x_2^s, \dots, x_m^s]$. Here, $x_1^s, x_2^s, \dots, x_m^s$ denote the enhanced learned representations obtained from each branch of DRIFA-Net. In this study, we address specific target tasks $y_t \in [0, 1, \dots, n]$, where n denotes the number of classes, involving both binary and multi-class

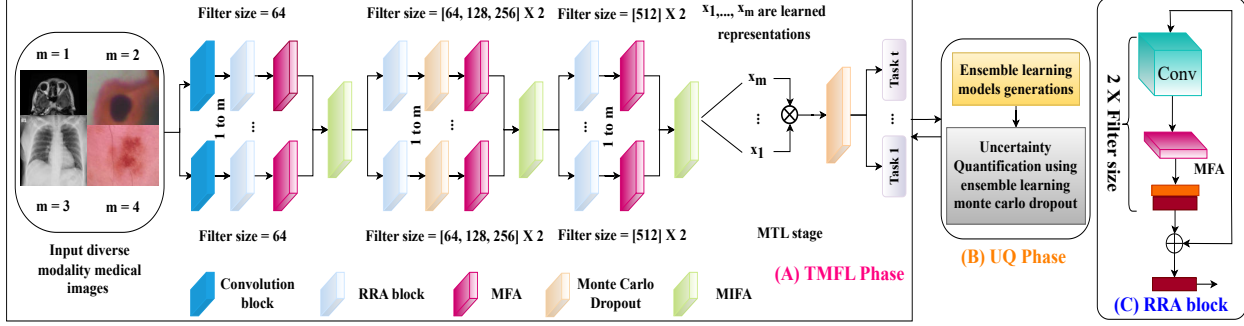


Figure 1. Detailed architecture of DRIFA-Net. Key components include: (A) the target-specific multimodal fusion learning (TMFL) phase, followed by (B) an uncertainty quantification (UQ) phase. TMFL phase comprises a robust residual attention (RRA) block, shown in (C), and utilizes multi-branch fusion attention (MFA), an additional MFA module for further refinement of local representations, a multimodal information fusion attention (MIFA) module for improved multimodal representation learning, and multitask learning (MTL) for handling multiple classification tasks. During (UQ) phase, the reliability of DRIFA-Net predictions are assessed.

classification problems across the diverse modalities present in our datasets.

3.1. Method Overview

Here we delve into the details of our proposed dual robust information fusion attention mechanism DRIFA.

We will show that it leverages information fusion learning with attention strategies across multimodal fusion learning settings, ensuring versatility and adaptability within diverse neural architectures. DRIFA is integrated with ResNet18, creating a multi-branch multimodal fusion learning network denoted as DRIFA-Net (depicted in Fig. 1). DRIFA method is detailed in Algorithm 1, which can be found in the supplementary materials. Each branch within ResNet18 incorporates input features from the corresponding modality, where ResNet18 structure consists of one convolutional block and eight residual blocks tailored to learn representations for each modality. In the following, we will discuss two salient phases of DRIFA-Net, i.e., – target-specific multimodal fusion learning (TMFL) and uncertainty quantification (UQ).

3.2. Target-specific Multimodal Fusion Learning

DRIFA-Net relies on target-specific multimodal fusion (TMFL), in pursuit of learning an enhanced shared multimodal representations to achieve better performance across target specific classification tasks. TMFL utilizes a robust residual attention (RRA) block, which incorporates our proposed multi-branch fusion attention (MFA) module, which effectively learns diverse refined local patterns. Additionally, TMFL also incorporates our proposed multimodal information fusion attention (MIFA) module to learn enhanced multimodal representations. Finally, a target-specific multitask learning (MTL) approach is used to handle multiple classification tasks simultaneously within

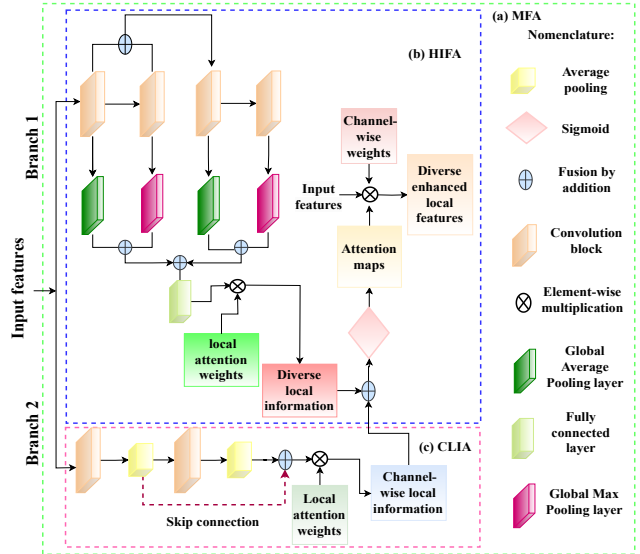


Figure 2. (a) Multi-branch fusion attention (MFA) module. Key components include hierarchical information fusion attention (HIFA) for diverse local information enhancement and channel-wise local information attention (CLIA) for improved channel-specific representation learning.

TMFL phase. In the following, we will discuss RRA, MIFA and MTL blocks – which represents salient elements of interest in TMFL.

3.2.1 RRA: Robust Residual Attention block

Let us in this section discuss RRA block which incorporates our proposed MFA module applied after each convolutional layer and utilizes a skip connection strategy. This approach aims to learn diverse local representations, thereby enhancing the performance of our learning network.

Multi-branch Fusion Attention Module (MFA) module

aims to learn enhanced local representations from input features. It is illustrated in Fig. 2. Specifically, the MFA module is integrated within each RRA block across all branches of the network. Another MFA module is employed to further refine these representations (Fig. 1 (a)), thereby improving the model’s ability to learn more detailed local patterns.

To enhance local information acquisition, MFA utilizes two attention modules:

- Hierarchical Information Fusion Attention (HIFA) module which enriches diverse local information, and
- Channel-Wise Local Information Attention (CLIA) module which compresses channel-wise information.

HIFA module is integrated into the first branch to capture diverse local features, while the CLIA module is applied in the second branch to refine channel-wise information, as shown in Figure 2. Additionally, a modulation strategy is employed to selectively emphasize critical representations in the input data and suppress irrelevant ones, thereby enhancing the overall performance of our learning network.

The MFA module aims to enhance diverse local representation learning by transforming input feature maps $x \in \mathbb{R}^{H \times W \times C}$, where H , W , and C denote the height, width, and number of channels respectively, to $x' = x \otimes a \otimes \omega_c$. Here, \otimes denotes element-wise multiplication, a is enhanced local attention maps, and ω_c is channel-wise learnable parameters that adjust the importance of each channel during training.

To design the HIFA module, we use p -th 1×1 convolution layers denoted as ψ_p , $\frac{p}{2}$ -th global average pooling (GAP) layers denoted as β , and $\frac{p}{2}$ -th global max pooling (GMP) layers denoted as γ for learning diverse local information. The process involves four key steps:

- First, input features are processed through a convolution layer and a GAP layer to capture initial local information $l_{p=0}$.
- Secondly, features from the p -th convolution layer are refined using a subsequent convolution layer and a GMP layer to extract additional local information $l_{p=1}$.
- Thirdly, the refined features are fused and passed through further convolution layers, each followed by either GAP or GMP, to capture diverse local information l_p .
- Finally, the resulting local information variants are hierarchically fused to obtain enhanced diverse local patterns. E.g., local information $l_{p=0}$ is fused with other local patterns $l_{p,p \neq 0}$ to learn enhanced diverse local information, followed by application of a fully connected layer f to compress these enhanced diverse information \hat{d} , as illustrated in Figure 2. This can be written as:

$$\begin{aligned} l_p &= \forall_p(\beta|\gamma) \circ (\Pi_p, \lambda_1, \lambda_2, \lambda_3), \text{ where} \\ \lambda_1 &= \psi_{(p+1)}(\Pi_p), \\ \lambda_2 &= \psi_{(p+2)}(\phi(\Pi_p, \lambda_1)), \\ \lambda_3 &= \psi_{(p+3)}(\lambda_2). \end{aligned} \tag{1}$$

Here, ϕ represents the fusion (addition) strategy, \forall_p denotes “for all p ”, Π_p represents $\psi_p(x)$, \circ denotes composition operator, and $|$ indicates either to employ the β layer or the γ layer after processing each components (as process), such as Π_p , λ_1 , λ_2 , and λ_3 to learn l_p .

$$\hat{d} = f(\forall_{l_p} [\varphi\{H_i, H_{i+1}\}]), \tag{2}$$

where φ denotes fusion (concatenation), \hat{d} represents diverse enhanced local information for each m , $H_i = \varphi(l_p, l_{p+1})$ and $H_{i+1} = \varphi(l_{p+2}, l_{p+3})$ such that $i = 0, 1$.

To design our CLIA module, we utilize q -th 1×1 convolution layers with sigmoid activation function (σ) followed by q th average pooling layer to compress channel information. Additionally, we use a skip connection strategy to fuse the resulting information with the initially compressed channel information, enhancing the learning of channel-wise local information and thereby improving our model’s performance, as we have:

$$\hat{l} = \phi(\delta_{q=1}(\eta_1), \delta_{q=2}(\eta_2)) \tag{3}$$

where δ denotes average pooling layer, \hat{l} represents enhanced local information i.e.,

$$\begin{aligned} \eta_1 &\in \sigma_{(q=1)}(\psi_{(q=1)}(x)), \\ \eta_2 &\in \sigma_{(q=2)}(\psi_{(q=2)}(\delta_{q=1}(\eta_1))). \end{aligned}$$

Finally, to combine the local information learned from HIFA and CLIA, we use learnable weights ω_d and ω_l to adjust the importance of each learned local information component that is \hat{d} and \hat{l} . Initially, ω_d is set to one and is multiplied with diverse enhanced local information \hat{d} to refine these patterns. Similarly, ω_l is set to one and multiplied with channel-wise enhanced local patterns \hat{l} to focus on refining channel-specific information. The refined information is then fused to enhance the capture of diverse local details. A sigmoid activation function σ is applied to generate attention maps a , which highlight crucial features and improve network performance by capturing fine-grained details, as shown in the following equation:

$$a = \sigma((\hat{d} \otimes \omega_d) + (\hat{l} \otimes \omega_l)). \tag{4}$$

These learnable weights in the MFA module are activated using a boolean value and are optimized through a back-propagation strategy, as detailed in the supplementary materials.

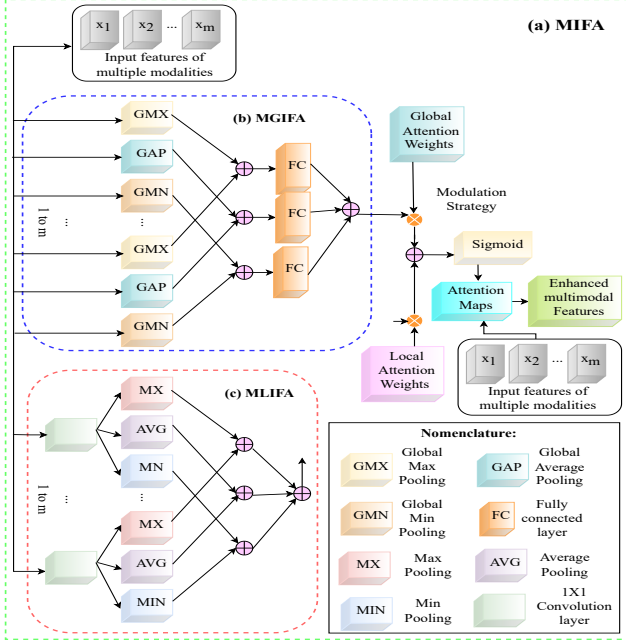


Figure 3. (a) Multimodal information fusion attention (MIFA) module. This module includes multimodal global information fusion attention (MGIFA) (shown in b) and multimodal local information fusion attention (MLIFA) (shown in c).

3.2.2 MIFA: Multimodal Information Fusion Attention Module

Let us discuss our proposed MIFA module in this section. The module is illustrated in Figure 3.

Given input feature maps from m heterogeneous modalities, $X \in x'_m$ (where x'_m denotes the enhanced local representations for each modality), the MIFA module aims to learn enhanced multimodal representations X^S .

This involves element-wise multiplication of multimodal shared attention maps A with input features X , and channel-wise learnable parameters w_{c_m} for each m , i.e.,

$$X^S = X \otimes A \otimes w_{c_m}. \quad (5)$$

These parameters work similarly to the channel-wise learnable parameters of the MFA module (subsection 3.2.1), i.e., w_{c_m} that adjust the importance of each channel during training. However, unlike MFA, which is applied to a single modality, these parameters are utilized across multiple modalities.

To learn multimodal shared attention feature maps A , we design two attention modules: the multimodal global information fusion attention (MGIFA) and the multimodal local information fusion attention (MLIFA). Additionally, we incorporate a fusion strategy similar to the MFA module.

Both MGIFA and MLIFA modules incorporate various pooling layers. For learning diverse global contexts – global

minimum pooling (α), global max pooling (γ), and global average pooling (β) are used. Whereas for learning diverse local fine-grained details – minimum pooling ϑ , max pooling τ , and average pooling δ are used.

To enhance the learning of diverse global and local information, we design the multimodal global and local information fusion (MGLIF) approach. Specifically, this approach fuses each pooling layer of one modality with corresponding similar pooling layers of other modalities to learn complementary information in both global and local contexts. The resulting complementary information enhances learning across all modalities in each branch of our learning network model, bolstering a better performance. For example, to enhance global information obtained from global average pooling, the learned global information from modality 1 is fused with the global information from the other $m - 1$ modalities. This strategy is applied uniformly across all information learned from respective pooling layers, aiming to achieve enhanced diversity in both global and local information. Furthermore, a fully connected layer f_{pool} is applied to each resulting information, followed by the fusion of all resulting information to learn enriched global g' and local representations l' – as shown in the following equation:

$$g' = \phi \left(f_{pool} \left(\sum_{i=1}^m G_{pool,i}(X) \right) \right) \quad (6)$$

$$l' = \phi \left(f_{pool} \left(\sum_{i=1}^m L_{pool,i}(X) \right) \right) \quad (7)$$

where $X \in x'_m$, $G_{pool} \in \{\alpha, \gamma, \beta\}$ and $L_{pool} \in \{\vartheta, \tau, \delta\}$.

Similar to the MFA module, to combine learned information (e.g., \hat{g} and \hat{l}) from MGIFA and MLIFA, we use learnable weights (w_{d_m} and w_{l_m}) to adjust the importance of this information, thereby refining the patterns. In multimodal fusion learning settings, a fusion operation (addition) followed by a sigmoid activation σ generates multimodal shared attention maps A , capturing diverse global contexts and fine-grained details:

$$A = \sigma((g' \otimes w_{d_m}) + (l' \otimes w_{l_m})). \quad (8)$$

3.2.3 MTL: Target-specific Multitask Learning

In the MTL stage, we utilize shared representations X^S from the TMFL phase across m diverse medical imaging modalities. This enhances DRIFA-Net's generalization capability by learning robust complementary information, thereby improving predictions on multiple modality-specific test sets. The MTL approach leverages DRIFA-Net $\theta(\cdot)$ to map input features $[x_1, \dots, x_m]$ from m modalities to t classification tasks $[y_1, \dots, y_t]$. The MTL loss function ∂_{MTL} combines task-specific cross-entropy losses ∂_t^m , as defined in the following as:

$$\partial_{\text{MTL}} = \sum_t \omega_t^m \times \partial_t^m(\theta(X^S, y_t)). \quad (9)$$

where $\theta(X^S, y_t) = [x_1, \dots, x_m] \rightarrow [y_1, \dots, y_t]$, and ω_t^m represents the weighting factor for each task-specific cross-entropy loss, ensuring efficient task performance balance.

3.3. Uncertainty Quantization

We assess the prediction uncertainty in DRIFA-Net using the ensemble Monte Carlo dropout strategy. This approach computes soft probabilities \hat{y} by averaging random predictions from z ensemble models, each utilizing stochastic sampling dropout masks (\aleph) to introduce randomness into DRIFA-Net. Our approach involves $e = 20$ iterations of Monte Carlo sampling to generate diverse predictions through $\theta(\cdot)$. During testing, DRIFA-Net is executed 20 times on multiple modality-specific test sets, and prediction uncertainty is inferred from the averaged results of these runs as shown in the following equation:

$$\hat{y} = \arg \max \left(\frac{1}{z} \sum_0^{z-1} [\Omega(\theta(X^S, \aleph))] \right), \quad (10)$$

where Ω represents a softmax classifier.

4. Experiments and Results

Datasets – Our experiments utilized five medical imaging datasets: HAM10000 [37], SIPaKMeD [30], Nickparvar MRI [26], IQ-OTHNCCD lung cancer [2], and BraTS2020 [24] (denoted as D1, D2, D3, D4, and D5 respectively). These datasets encompass diverse modalities: dermoscopy, single-cell pap smear, MRI, and CT-scan. HAM10000 comprises 10,015 images across seven classes, SIPaKMeD includes 4,049 images over five classes, Nickparvar contains 7,023 MRI images across four classes, and the IQ-OTHNCCD lung cancer dataset has 1,098 images in three classes. The BraTS2020 dataset comprises four MRI modalities: fluid-attenuated inversion recovery (FLAIR), T1-weighted (T1), T1-weighted contrast-enhanced (T1ce), and T2-weighted (T2) imaging. It includes 369 training subjects, which are randomly split into 201 for training, 35 for validation, and 133 for testing. The BraTS2020 challenge provides ground truth annotations for the imaging data, evaluating three sub-regions: whole tumor (WT), tumor core (TC), and enhancing tumor (ET). Data augmentation techniques, such as rotation and transformation, ensured uniformity in sample size for multimodal fusion learning operations. All images were resized to $128 \times 128 \times 3$ pixels, with an 80% training, 10% validation, and 10% testing split.

Models – We compare the performance of DRIFA-Net with state-of-the-art (SOTA) methods across four datasets

(D1–D4) for classifying skin cancer, cervical cancer, brain tumors, and lung cancer, as well as one dataset (D5) for brain tumor segmentation tasks. Specifically, we employ approaches such as Gloria [15], MTTU-Net [9], CAF [13], and MTF with MA [6] (denoted as M1, M2, M3, M4 respectively). Note, DRIFA-Net is denoted as M5. We reconfigure these methods according to our multimodal fusion learning settings to ensure an accurate and consistent performance comparison.

Notation – In our results, Acc denotes accuracy, Prec represents precision, Rec stands for recall, F1 refers to the F1 score, SN indicates sensitivity, and SP represents specificity.

Implementations Details – Implementations were executed on an NVIDIA GeForce RTX 4060 Ti GPU. Models were trained for 200 epochs using cross-entropy loss with a batch size of 32. The Adam optimizer was used with an initial learning rate of 0.001. A Reduce Learning Rate on Plateau scheduler was employed, reducing the rate by a factor of 0.2 after 5 epochs of no improvement, with a minimum learning rate of 10^{-5} . For uncertainty quantification, we adopted the ensemble Monte Carlo dropout method, generating five ensemble models with a dropout rate of 0.25. In this study, all learnable parameters, including ω_c , ω_d , ω_l , ω_{dm} , ω_{lm} , and ω_{cm} , are initialized to 1 and can be adjusted during training based on gradients computed from the MTL loss function ∂_{MTL} .

4.1. Performance Comparison with SOTA Methods

In summary, DRIFA-Net achieved a remarkable performance between 95.4% and 99.7% when evaluated on four diverse medical imaging datasets (D1–D4). In the following, let us delve down deeply in the results. The experimental results presented in Table 1 indicate that our proposed method surpassed all state-of-the-art multimodal fusion learning approaches, resulting in significant performance enhancements. Specifically, our method shows notable improvements across all metrics used, including accuracy, precision, recall, and F1-score, with gains ranging from 0.2% to 11.4% over other SOTA models.

Additionally, we applied our DRIFA method to the Inception-v3 network [34] and SegNet [5] to evaluate its performance when integrated with these architectures on the D1{D4} datasets and the D5 dataset, respectively. The results are shown in Tables 2 and 3 respectively. DRIFA-Net demonstrated significant performance improvements of 1.1% to 3.2% over the leading state-of-the-art multimodal fusion learning methods on the D1{D4} datasets with Inception-v3 network (Table 2). It also achieved strong results on the D5 dataset, with performance gains ranging from 1.4% to 5% compared to the top competitive model – M2, on SegNet model (Table 3) on BraTS2020 dataset.

Table 1. Performance comparison of our proposed DRIFA-Net (M5) with existing multimodal fusion learning approaches (M1-M4) on four benchmark datasets (D1-D4).

Dataset	Method	Acc	Prec	Rec	F1	Dataset	Method	Acc	Prec	Rec	F1
D1	M1	97.9	88.5	84.8	86.5	D2	M1	95.1	95.1	95.1	95.1
	M2	97.4	95.5	97.4	96.5		M2	91.9	92.5	92.1	92.3
	M3	97.2	95.9	98	97.2		M3	91	91.5	91.5	91.5
	M4	94.4	94.2	93.8	93.8		M4	95.08	95.06	95.1	95.06
	M5	98.2	96.4	99.5	97.9		M5	95.6	95.6	95.4	95.5
D3	M1	98.1	98.2	96.3	97.5	D4	M1	91.5	98.8	97.8	98.3
	M2	97.9	98.0	99.8	98.0		M2	99.5	99.5	99.0	99.2
	M3	97.2	97.0	97.0	97.0		M3	98.7	97.5	97.2	97.2
	M4	97.4	98.3	96.9	97.3		M4	98.2	98.3	98.2	98.1
	M5	98.4	98.4	98.4	98.4		M5	99.7	99.7	99.3	99.5

Table 2. Performance comparison of our proposed DRIFA approach integrated with Inception-v3 model, named DRIFA-Net (M5) with existing multimodal fusion learning approaches (M1-M4) on four benchmark datasets (D1-D4).

Dataset	Method	Acc	F1	AUC	Dataset	Method	Acc	F1	AUC
D1	M1	97.9	91.5	95.4	D2	M1	95.5	95.5	95.9
	M2	96.5	96.3	96.5		M2	92.8	92.8	93.5
	M3	97.1	94.5	96.8		M3	91.7	92.3	92.8
	M4	95.3	94.7	95.8		M4	94.8	95.1	95.5
	M5	100	100	100		M5	98.1	98.1	98.9
D3	M1	96.8	96.5	96.5	D4	M1	93.7	96.4	95.2
	M2	96.8	96.05	96.5		M2	98.1	97.8	98.1
	M3	96.3	95.9	96.4		M3	98.5	98.2	98.1
	M4	96.5	96.3	96.3		M4	97.8	97.8	98
	M5	97.9	97.7	98.5		M5	99.7	99.7	99.5

Table 3. Performance comparison of our proposed DRIFA approach is integrated with SegNet model, named DRIFA-Net (M5) with existing multimodal fusion learning approaches (M1-M4) on BraTS2020 dataset.

Method	Dice Score (%)				Average Performance			
	WT	TC	ET	Average	Acc	AUC	SN	SP
M1	85.3	79.8	75.6	80.2	86.2	84.4	80.6	89.7
M2	89.9	85.1	79.8	84.9	90.5	86.9	84.8	92.5
M3	85.7	80.2	77.1	81	86.8	84.9	81.1	90.5
M4	84.5	78.5	75.2	79.4	85.9	82.8	79.9	88.02
M5	93.6	90.5	85.6	89.9	93.6	90.14	88.6	93.9

As we discussed earlier, our method excels over existing approaches due to their limited applicability across diverse medical imaging modalities, such as dermoscopy, pap smear cell images, MRI, and CT-scan. These methods often fail to harness the benefits of multiple domains, restricting their ability to capture robust multimodal information and thereby improve model performance. For the D5 dataset, the existing M2 approach performs well but still achieves limited results due to its lack of focus on leveraging multiple attention methods for enhanced representation learning. Our approach addresses these limitations by integrating multiple attention methods (MFA and MIFA) to enhance modality-specific and multimodal representation learning, achieving significant performance gains.

4.2. Ablation Study

We evaluated the impact of different components of our proposed DRIFA method on two benchmark datasets D1 and D2 [30,37] – focusing on MFA and MIFA modules. The results are given in Table 4. It can be seen that DRIFA approach incorporating both modules outperformed versions employing only one component, achieving performance enhancements ranging from 0.5% to 10%. This

Table 4. Comparative evaluation of MFA (multi-branch fusion attention) and MIFA (multimodal information fusion attention) components in DRIFA – showcasing significant performance enhancement on two benchmark datasets D1 and D2.

Dataset	MFA	MIFA	Method	Acc	Prec	Rec	F1
D1	x	x	DRIFA-Net (Baseline)	94.85	94.4	95.2	94.7
	✓	x	DRIFA-Net + MFA	95.9	95.8	96.5	96.2
	x	✓	DRIFA-Net + MIFA	96.3	96.3	96.8	96.6
	✓	✓	DRIFA-Net + MFA + MIFA	98.2	96.4	99.5	97.9
	x	x	DRIFA-Net	90.1	88.7	89.2	88.9
D2	✓	x	DRIFA-Net + MFA	93.8	93.6	93.8	93.8
	x	✓	DRIFA-Net + MIFA	92.7	93.5	94.7	94.2
	✓	✓	DRIFA-Net + MFA + MIFA	95.6	95.6	95.4	95.5
	x	x	DRIFA-Net	90.1	88.7	89.2	88.9
	✓	✓	DRIFA-Net + MFA + MIFA	93.8	93.6	93.8	93.8

Table 5. Experimental evaluation of each DRIFA component—HIFA, CLIA, MGIFA, and MLIFA—on performance by adding and removing them, using datasets D1 and D2.

Dataset	HIFA	CLIA	MGIFA	MLIFA	Accuracy	Precision	Recall	F1 score
D1	x	x	x	x	94.8	94.4	95.2	94.7
	✓	x	✓	x	95.7	95.7	95.9	95.7
	x	✓	x	✓	95.1	95.1	94.9	94.9
	✓	✓	✓	✓	98.2	96.4	99.5	97.9
	x	x	x	x	90.1	88.7	89.2	88.9
D2	✓	x	✓	x	93.2	93.2	93.5	93.2
	x	✓	x	✓	91.9	91.9	92.2	92
	✓	✓	✓	✓	95.6	95.6	95.4	95.5
	x	x	x	x	90.1	88.7	89.2	88.9
	✓	✓	✓	✓	93.2	93.2	93.5	93.2

Table 6. Experimental evaluation on the impact of parameters ω_d , ω_l , ω_c for MFA (Eq. 4), and ω_{d_m} , ω_{l_m} , ω_{c_m} for MIFA (Eq. 8) with benchmark dataset D1.

ω_d	ω_l	ω_c	Method	Acc	F1	ω_{d_m}	ω_{l_m}	ω_{c_m}	Method	Acc	F1
✓	✓	✓	DRIFA-Net+MFA	94.85	94.7	✓	✓	✓	DRIFA-Net+MIFA	94.85	94.7
✓	✓	✓		95.21	95.18	✓	✓	✓		95.30	95.4
✓	✓	✓		95.47	95.62	✓	✓	✓		95.85	96.0
✓	✓	✓		95.80	96.05	✓	✓	✓		95.99	96.2
✓	✓	✓		95.57	95.83	✓	✓	✓		96.05	96.43
✓	✓	✓		95.90	96.20	✓	✓	✓		96.3	96.6

demonstrated the effectiveness and efficacy of our proposed modules. Again as discussed earlier, this superiority stems from leveraging distinct attention mechanisms for enhancing modality-specific representations and improving multimodal shared representations simultaneously.

We assessed the impact of each component within the attention modules, specifically, the HIFA and CLIA components of the multi-branch fusion attention module, and the MGIFA and MLIFA components of the multimodal information fusion attention module. These evaluations are done on two benchmark datasets D1 and D2, and the results are shown in Table 5. The experimental results demonstrate that our proposed DRIFA approach, incorporating all attention components, significantly outperforms versions utilizing at most one component to at least one component, with performance improvements ranging from 0.7% to 5.5%. One can infer that the limited performance of approaches using only one component arises due to their focus on either enhancing single-modal or multimodal local information, or diverse multimodal global information from modality-specific input features. In contrast, (as discussed earlier) our proposed DRIFA approach designs one attention mechanism for modality-specific representation learning and another for improving multimodal shared representation learning. This strategy enhances multimodal representation learning across both global and local contexts in the input data, lead-

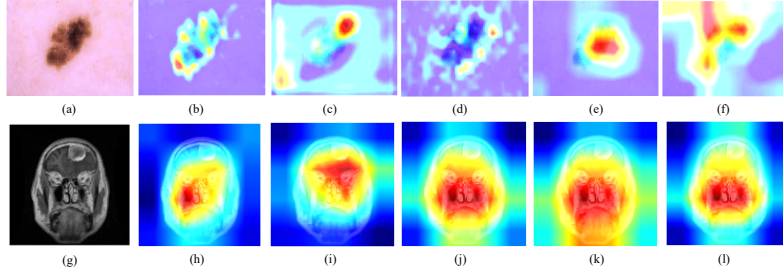


Figure 4. Visual representation of the important regions highlighted by our proposed DRIFA-Net and four SOTA methods using the GRAD-CAM technique on two benchmark datasets D1 and D3. (a) and (g) display the original images, while (b) and (h) present results for Gloria, (c) and (i) for MTF with MA, (d) and (j) for CAF, (e) and (k) for MTU-Net, and (f) and (l) for our proposed DRIFA-Net.

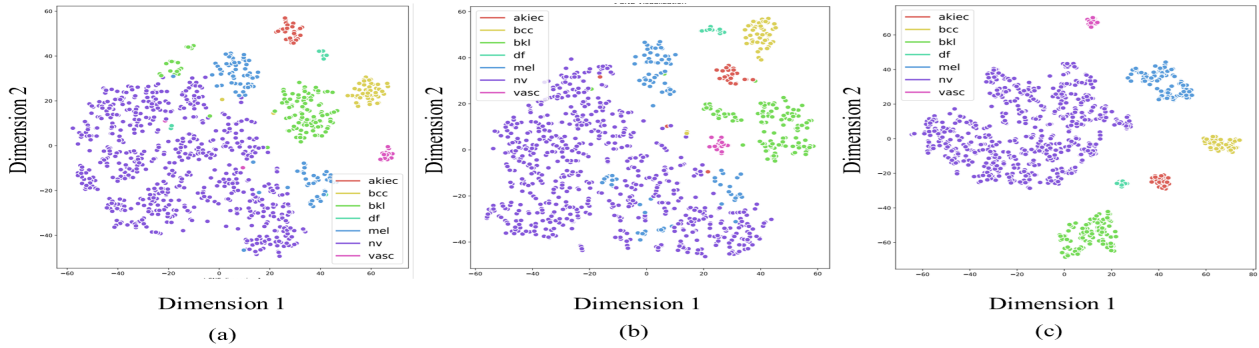


Figure 5. T-SNE visualization of different models applied to the dermoscopy images of the D1 dataset, where (a) represents the T-SNE visualization of Gloria, (b) of MTU-Net, and (c) of our proposed DRIFA-Net.

Table 7. Uncertainty quantification of DRIFA-Net predictions on two benchmark datasets D1 and D2. DRIFA-Net + UQ denotes DRIFA with uncertainty quantification.

Dataset	Method	Accuracy	Precision	Recall	F1
D1	DRIFA-Net + UQ	97.5	95.6	98.9	97.3
D2	DRIFA-Net + UQ	95.1	95.2	94.9	95.05
D1	DRIFA-Net	98.2	96.4	99.5	97.9
D2	DRIFA-Net	95.6	95.6	95.4	95.5

ing to superior performance.

Finally, we evaluate the performance of DRIFA-Net + MFA on D1 dataset with the inclusion and exclusion of learnable parameters $\omega_d, \omega_l, \omega_c$, as discussed in Eq. 4 in Section 3.2.1, and shown in Table 6. We also compare the performance of DRIFA-Net + MIFA on D1 dataset with the inclusion and exclusion of $\omega_{d_m}, \omega_{l_m}, \omega_{c_m}$, discussed in Eq. 8 in Section 3.2.2 and shown in Table 6. It can be seen that the best performance is achieved on D1 dataset when the three components are included highlighting their efficacy and important role towards the working of DRIFA-Net + MFA and DRIFA-Net + MIFA.

4.3. Impact of uncertainty quantification

We utilized an ensemble Monte Carlo dropout (MCD) strategy to assess the prediction uncertainty of our proposed approach across each medical imaging modality, as detailed in Table 7. DRIFA with uncertainty quantification is denoted as DRIFA-Net + UQ and led to a marginal drops of 0.4% to 0.7% on the two benchmark datasets when compared to our model without uncertainty estimation. While

UQ can be computationally intensive, it was chosen for its reliability and flexibility. It handles various models without strong assumptions, providing a comprehensive view of outcomes and robust uncertainty estimation, crucial for accurate clinical decision-making.

4.4. Impact of qualitative analysis

We performed a qualitative analysis using Grad-CAM to assess the efficacy of our proposed method. This visualization highlighted regions of highest importance in the two benchmark datasets D1 and D3, as shown in Fig. 4. Additionally, the T-SNE plot for the D1 dataset in Fig. 5 further validated our model’s decisions by emphasizing areas crucial to the prediction scores.

5. Conclusion

In this paper, we proposed a dual information fusion attention approach to enhance multimodal fusion learning, making it applicable to diverse disease classification tasks across medical imaging modalities such as cervical, skin, lung cancer, and brain tumors. By combining multi-branch fusion attention and multimodal information attention modules, we outperform existing state-of-the-art methods shown through extensive experiments. Future work will focus on expanding our approach for more medical imaging modalities and optimizing computational efficiency.

References

- [1] I. S. A. Abdelhalim, M. F. Mohamed, and Y. B. Mahdy. Data augmentation for skin lesion using self-attention based progressive generative adversarial network. *Expert Systems with Applications*, 165:113922, 2021. [1](#)
- [2] Hamdalla Alyasriy and A Muayed. The iq-othnccd lung cancer dataset. *Mendeley Data*, 1(1):1–13, 2020. [2](#), [6](#)
- [3] Salha M. Alzahrani. Convattenmixer: Brain tumor detection and type classification using convolutional mixer with external and self-attention mechanisms. *Journal of King Saud University-Computer and Information Sciences*, 35(10):101810, 2023. [2](#)
- [4] V. Anand, S. Gupta, D. Koundal, and K. Singh. Fusion of u-net and cnn model for segmentation and classification of skin lesion from dermoscopy images. *Expert Systems with Applications*, 213:119230, 2023. [1](#), [2](#)
- [5] Vijay Badrinarayanan, Alex Kendall, and Roberto Cipolla. Segnet: A deep convolutional encoder-decoder architecture for image segmentation. *IEEE transactions on pattern analysis and machine intelligence*, 39(12):2481–2495, 2017. [6](#)
- [6] G. Cai, Y. Zhu, Y. Wu, X. Jiang, J. Ye, and D. Yang. A multimodal transformer to fuse images and metadata for skin disease classification. *The Visual Computer*, 39(7):2781–2793, 2023. [1](#), [2](#), [6](#)
- [7] Muhammed Celik and Ozkan Inik. Development of hybrid models based on deep learning and optimized machine learning algorithms for brain tumor multi-classification. *Expert Systems with Applications*, 238:122159, 2024. [1](#)
- [8] Q. Chen, M. Li, C. Chen, P. Zhou, X. Lv, and C. Chen. Mdfnet: application of multimodal fusion method based on skin image and clinical data to skin cancer classification. *Journal of Cancer Research and Clinical Oncology*, 149(7):3287–3299, 2023. [2](#)
- [9] J. Cheng, J. Liu, H. Kuang, and J. Wang. A fully automated multimodal mri-based multi-task learning for glioma segmentation and idh genotyping. *IEEE Transactions on Medical Imaging*, 41(6):1520–1532, June 2022. [1](#), [2](#), [6](#)
- [10] J. Dhar. An adaptive intelligent diagnostic system to predict early stage of parkinson’s disease using two-stage dimension reduction with genetically optimized lightgbm algorithm. *Neural Computing and Applications*, 34(6):4567–4593, 2021. [1](#)
- [11] M. I. Georgescu, R. T. Ionescu, A. I. Miron, O. Savencu, N. C. Ristea, N. Verga, and F. S. Khan. Multimodal multi-head convolutional attention with various kernel sizes for medical image super-resolution. In *Proceedings of the IEEE/CVF winter conference on applications of computer vision*, pages 2195–2205, 2023. [1](#), [2](#)
- [12] Q. Han, X. Qian, H. Xu, K. Wu, L. Meng, Z. Qiu, and X. Gao. Dm-cnn: Dynamic multiscale convolutional neural network with uncertainty quantification for medical image classification. *Computers in Biology and Medicine*, 168:107758, 2024. [1](#), [2](#)
- [13] X. He, Y. Wang, S. Zhao, and X. Chen. Co-attention fusion network for multimodal skin cancer diagnosis. *Pattern Recognition*, 133:108990, 2023. [1](#), [2](#), [6](#)
- [14] K. Hemalatha, V. Vetriselvi, and M. Dhandapani. Cervix-fuzzyfusion for cervical cancer cell image classification. *Biomedical Signal Processing and Control*, 85:104920, 2023. [1](#), [2](#)
- [15] S. C. Huang, L. Shen, M. P. Lungren, and S. Yeung. Gloria: A multimodal global-local representation learning framework for label-efficient medical image recognition. In *Proceedings of the IEEE/CVF International Conference on Computer Vision*, pages 3942–3951, 2021. [1](#), [2](#), [6](#)
- [16] M. M. Islam and T. Iqbal. Mumu: Cooperative multitask learning-based guided multimodal fusion. In *Proceedings of the AAAI Conference on Artificial Intelligence*, volume 36, pages 1043–1051, June 2022. [1](#), [2](#)
- [17] Jeremy Kawahara, Seyed Daneshvar, Giuseppe Argenziano, and Ghassan Hamarneh. Seven-point checklist and skin lesion classification using multitask multimodal neural nets. *IEEE journal of biomedical and health informatics*, 23(2):538–546, 2018. [2](#)
- [18] Y. Kihara, G. Montesano, A. Chen, N. Amerasinghe, C. Dimitriou, A. Jacob, and A. Y. Lee. Policy-driven, multimodal deep learning for predicting visual fields from the optic disc and oct imaging. *Ophthalmology*, 129(7):781–791, 2022. [2](#)
- [19] S. Kim, T. G. Purdie, and C. McIntosh. Cross-task attention network: Improving multitask learning for medical imaging applications. In *International Conference on Medical Image Computing and Computer-Assisted Intervention*, pages 119–128. Springer Nature Switzerland, 2023. [1](#), [2](#)
- [20] Y. Li, J. Zhao, Z. Lv, and Z. Pan. Multimodal medical supervised image fusion method by cnn. *Frontiers in Neuroscience*, 15:638976, 2021. [2](#)
- [21] Y. Ling, Y. Wang, W. Dai, J. Yu, P. Liang, and D. Kong. Mtanet: Multitask attention network for automatic medical image segmentation and classification. *IEEE Transactions on Medical Imaging*, 2023. [1](#), [2](#)
- [22] W. Liu, C. Li, M. M. Rahaman, T. Jiang, H. Sun, X. Wu, and M. Grzegorzec. Is the aspect ratio of cells important in deep learning? a robust comparison of deep learning methods for multiscale cytopathology cell image classification: From convolutional neural networks to visual transformers. *Computers in biology and medicine*, 141:105026, 2022. [2](#)
- [23] A. Manna, R. Kundu, D. Kaplun, A. Sinitca, and R. Sarkar. A fuzzy rank-based ensemble of cnn models for classification of cervical cytology. *Scientific Reports*, 11(1):14538, 2021. [2](#)
- [24] Bjoern H Menze, Andras Jakab, Stefan Bauer, Jayashree Kalpathy-Cramer, Keyvan Farahani, Justin Kirby, Yuliya Burren, Nicole Porz, Johannes Slotboom, Roland Wiest, et al. The multimodal brain tumor image segmentation benchmark (brats). *IEEE transactions on medical imaging*, 34(10):1993–2024, 2014. [2](#), [6](#)
- [25] A. Naveed, S. S. Naqvi, T. M. Khan, and I. Razzak. Pca: Progressive class-wise attention for skin lesions diagnosis. *Engineering Applications of Artificial Intelligence*, 127:107417, 2024. [1](#), [2](#)
- [26] Msoud Nickparvar. Brain tumor MRI dataset. Data set, 2021. Accessed on 3rd March. [2](#), [6](#)

- [27] A. N. Omeroglu, H. M. Mohammed, E. A. Oral, and S. Aydin. A novel soft attention-based multimodal deep learning framework for multi-label skin lesion classification. *Engineering Applications of Artificial Intelligence*, 120:105897, 2023. 1, 2
- [28] I. Pacal and S. K?l?carslan. Deep learning-based approaches for robust classification of cervical cancer. *Neural Computing and Applications*, 35(25):18813–18828, 2023. 2
- [29] R. Pedro and A. L. Oliveira. Assessing the impact of attention and self-attention mechanisms on the classification of skin lesions. In *2022 International Joint Conference on Neural Networks (IJCNN)*, pages 1–8. IEEE, 2022. 1, 2
- [30] Maria E Plissiti, Panagiotis Dimitrakopoulos, Giorgos Sfikas, Christophoros Nikou, Orestis Krikoni, and Avraam Charchanti. Sipakmed: A new dataset for feature and image based classification of normal and pathological cervical cells in pap smear images. In *2018 25th IEEE International Conference on Image Processing (ICIP)*, pages 3144–3148. IEEE, October 2018. 2, 6, 7
- [31] S. Qian, K. Ren, W. Zhang, and H. Ning. Skin lesion classification using cnns with grouping of multiscale attention and class-specific loss weighting. *Computer Methods and Programs in Biomedicine*, 226:107166, 2022. 1, 2
- [32] Y. Song, J. Zou, K. S. Choi, B. Lei, and J. Qin. Cell classification with worse-case boosting for intelligent cervical cancer screening. *Medical Image Analysis*, 91:103014, 2024. 2
- [33] S. Steyaert, M. Pizurica, D. Nagaraj, P. Khandelwal, T. Hernandez-Boussard, A. J. Gentles, and O. Gevaert. Multimodal data fusion for cancer biomarker discovery with deep learning. *Nature Machine Intelligence*, 5(4):351–362, 2023. 1
- [34] Christian Szegedy, Vincent Vanhoucke, Sergey Ioffe, Jon Shlens, and Zbigniew Wojna. Rethinking the inception architecture for computer vision. In *Proceedings of the IEEE conference on computer vision and pattern recognition*, pages 2818–2826, 2016. 6
- [35] S. Tabarestani, M. Aghili, M. Eslami, M. Cabrerizo, A. Barreto, N. Rische, and M. Adjouadi. A distributed multitask multimodal approach for the prediction of alzheimer’s disease in a longitudinal study. *NeuroImage*, 206:116317, 2020. 2
- [36] K. Tan, W. Huang, X. Liu, J. Hu, and S. Dong. A multimodal fusion framework based on multi-task correlation learning for cancer prognosis prediction. *Artificial Intelligence in Medicine*, 126:102260, 2022. 2
- [37] Philipp Tschandl, Cliff Rosendahl, and Harald Kittler. The ham10000 dataset, a large collection of multi-source dermatoscopic images of common pigmented skin lesions. *Scientific data*, 5(1):1–9, 2018. 2, 6, 7
- [38] A Vaswani. Attention is all you need. *Advances in Neural Information Processing Systems*, 2017. 1
- [39] L. Yang, C. Fan, H. Lin, and Y. Qiu. Rema-net: An efficient multi-attention convolutional neural network for rapid skin lesion segmentation. *Computers in Biology and Medicine*, 159:106952, 2023. 1, 2
- [40] A. Z. Yutra, J. Zheng, X. Li, and A. Endris. Skinaacn: An efficient skin lesion classification based on attention augmented convnext with hybrid loss function. In *Proceedings of the 2023 7th International Conference on Computer Science and Artificial Intelligence*, pages 295–300, 2023. 1, 2
- [41] L. Zhou and Y. Luo. Deep features fusion with mutual attention transformer for skin lesion diagnosis. In *2021 IEEE international conference on image processing (ICIP)*, pages 3797–3801. IEEE, 2021. 1, 2